

Phonon-electron interaction and vibration correlations in germanium within a broad temperature interval

A. Kirfel and J. Grybos

Mineralogisch-Petrologisches Institut der Universität Bonn, Poppelsdorfer Schloss, D-53115 Bonn, Germany

V. E. Dmitrienko

A.V. Shubnikov Institute of Crystallography, 117333 Moscow, Russia

(Received 04 April 2002; published 2 October 2002)

The temperature dependence of the “forbidden” reflection 006 in a germanium single crystal was studied from 299 to 735 K using x-ray resonant scattering at the K -absorption edge. Since the intensity is found to increase by a factor of almost 8 for the maximum temperature, the reflection intensity is dominated by phonon-electron interactions. A theory is developed, which relates the “forbidden” reflection intensity to the vibration correlations, u_{\parallel}^2 and u_{\perp}^2 , of neighboring atoms, and it is inferred that u_{\parallel}^2 provides the main contribution to the thermal-motion-induced anisotropy of x-ray resonant scattering.

DOI: 10.1103/PhysRevB.66.165202

PACS number(s): 61.10.-i

I. INTRODUCTION

Electron-phonon interaction was extensively investigated for many decades¹ because of its importance for solid-state conductivity, superconductivity, etc. In crystals, electrons (or holes) distort the surrounding lattice, and these distortions can be described as phonons. There should also be an opposite effect which could be called *phonon-electron* interaction, i.e., thermal phonons distort the configurational environment of an atom and hence distort its electronic states. Indeed, since the atomic motion is much slower than that of an electron, the electronic states always correspond to the instantaneous atomic configuration (the so-called adiabatic or Born-Oppenheimer approximation). However, this effect should be rather small due to the large difference between the typical energies (few eV for valence electron states and a few meV for thermal phonons). Consequently, one needs a very sensitive method to detect such small distortions of the electronic states induced by thermal motion. Such a method was first suggested theoretically^{2,3} and then proved experimentally.^{4,5} The basic idea is that the thermal motion should violate the point symmetry of an atomic environment and that the corresponding distortions of the electronic states should result in an anisotropy of the x-ray susceptibility, which consequently results in a special type of “forbidden” Bragg reflection.

It has been known for many years⁶ that an anisotropy of the x-ray susceptibility allows the excitement of reflections otherwise forbidden by screw-axis or glide-plane symmetry operations. After the theoretical development^{7,8} and the first experimental observation^{9,10} of such “forbidden” reflections in NaBrO_3 , similar reflections were studied in many other crystals, e.g., in Cu_2O ,¹¹ TiO_2 , MnF_2 ,¹² $\text{Ba}(\text{BrO}_3)_2 \times \text{H}_2\text{O}$,¹³ Fe_3O_4 ,¹⁴ FeS_2 ,¹⁵ and $\text{La}_{0.5}\text{Sr}_{1.5}\text{MnO}_4$ (Ref. 16) (orbital ordering). In all these cases, the dipole-dipole anisotropies of the x-ray susceptibility arise near the absorption edges of resonant scattering atoms because the electronic states of these atoms are distorted by their asymmetric environments.

A more intriguing situation occurs when a resonant atom occupies a position with so high a symmetry that the dipole-

dipole anisotropy is absent (as in the germanium structure where the symmetry of the equilibrium atomic position is $\bar{4}3m$). In this case, “forbidden” reflections can be excited owing to a higher-rank-tensor anisotropy. For example, in Ge, $0kl, k+l=4n+2$ reflections can appear as a consequence of a mixed dipole-quadrupole transition.¹⁷ However, there is also another physical mechanism which can be responsible for the excitement of those reflections.^{2,3} That is, if the resonant atom leaves its equilibrium position in arbitrary direction, then the point symmetry of its instantaneous environment is lowered, its electronic wave functions become distorted, and the dipole-dipole anisotropy can again apply. Contrary to the first described situation, which results in an intensity decrease with increasing temperature, as observed for cuprates,¹⁸ a thermal-motion-induced (TMI) anisotropy is expected to grow (in absolute value) with rising temperature. For germanium, it was shown⁴ that the latter effect gives the main contribution to the intensity of the $00l, l=4n+2$ reflections, even at room temperature. The fact that at low temperatures a temperature-independent contribution was found might be attributed to either a dipole-quadrupole anisotropy or to other static effects.

In this paper, the study of the temperature dependence of the “forbidden” 006 reflection in germanium is extended to higher temperatures. Intensity, resonant energy, and resonance width are measured and carefully analyzed from 299 to 735 K. In addition, the theory is significantly improved by taking into account the vibration correlations, u_{\parallel}^2 and u_{\perp}^2 , parallel and perpendicular to the bonds between neighboring atoms.

In this context, it may be noticed that the measured intensity of a TMI reflection includes both elastic and inelastic coherent scattering (the latter is accompanied by absorption or creation of phonons). The energy of the diffracted x rays was not analyzed in our experiment, and values below the difference between elastic and inelastic scattering will be ignored. Potentially, recording both contributions could supply the same information about electronic states as the resonant inelastic x-ray scattering¹⁹ plus special data on phonon vibra-

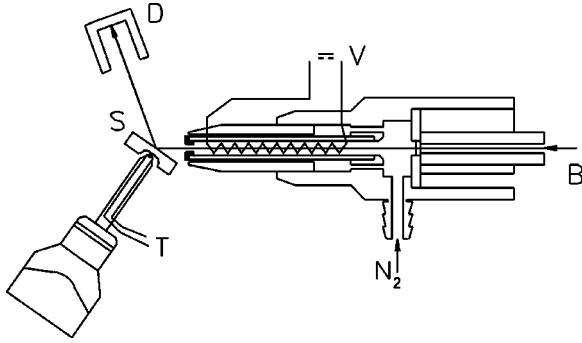


FIG. 1. Experimental setup. S=sample, T=thermocouple, D=detector, B=sprimary beam, C=collimator, and V=power supply.

tions. For instance, with TMI reflections, we could study not only phonon eigenfrequencies but also phonon eigenvectors because the relative mean-square displacements of the atoms, u_{\parallel}^2 and u_{\perp}^2 , are very sensitive to the eigenvectors.²⁰ Since information about the eigenvectors is hardly accessible with neutron scattering,²¹ any new method to obtain it would be very useful.

II. EXPERIMENT

Experiments were carried out on the four-circle diffractometer installed at beam line D3 at HASYLAB, Hamburg,^{22,23} DORIS being operated at 4.5 GeV, maximum current 140 mA. The instrument is equipped with a fixed exit double-crystal-type Si(111) monochromator with an energy resolution of 4×10^{-4} at 12 keV.

The sample was a $5 \times 5 \times 1$ mm³ (001) cut of a Ge single crystal. This wafer, containing on one side a drill hole of about 0.5-mm depth in order to house the joint of a chromel-alumel thermocouple, was flat mounted on top of a corundum tube with two channels through which the thermocouple wires were led outside. Thus, the crystal temperature could be continuously monitored during the measurements, which were made in symmetrical Bragg geometry illuminating the intact (001) face with a beam of 0.8-mm diameter.

Heating of the sample was achieved by a N₂ gas-stream heater²⁴ coaxially mounted on the primary beam collimator so that the x-ray beam and the gas stream coincided (Fig. 1). The distance between the sample surface and the heater nozzle was 4 mm. The ensuing experimental procedure consisted of several steps:

(i) Establishment of the orientation matrix at $E = 11.080$ keV, right below the Ge *K*-absorption edge, using 24 reflections, 001 and adjacent *hkl*.

(ii) Calibration of the monochromator to the middle of the absorption edge ($E_a = 11.104$ keV) according to the Ge-fluorescence yield and starting the search for the “forbidden” reflection 006.

(iii) Once $I(006)$ was observed, the maximum resonance energy was determined by measuring $I(006)$ as a function of the energy E in steps of $\Delta E = 1$ eV.

(iv) At this energy, measurements of $I(006; \Psi)$ using ω scans and steps of $\Delta \Psi = 15^\circ$ over a 270° range. The ob-

served intensities clearly showed the expected modulation with $\pi/2$ periodicity, i.e., the signal was proved to be due to the excitement of 006 rather than due to an “umweganregung.”

(v) Choosing three Ψ settings at 35° , 40° , and 48° , close to the intensity maximum at $\Psi = 45^\circ$, $I(006; \Psi)$ values were once more recorded by ω scans (91 steps, $\Delta \omega = 0.003^\circ$, 2 sec/step) as a function of energy using steps of 1 eV. The three Ψ settings were necessary in order to improve the counting statistics and, more important, to ensure that occasional “umweganregungen” could be detected and eliminated from the data.

(vi) In the following, steps i and v were repeated after raising the crystal temperature to 373, 475, 523, 573, 623, 673, and 700 K, respectively. Thus, in total, eight resonance curves were determined at increasing temperatures, for each using three Ψ settings per energy step of $\Delta E = 1$ eV.

In order to correct the temperature readings recorded during the experiment for a possible temperature gradient normal to the sample surface, the experimental situation was later simulated in the home laboratory where the temperature in the drill hole could be correlated with that measured by another thermocouple contacting the sample surface at one edge. According to these measurements the experimental temperatures were corrected to 299, 384, 493, 547, 601, 654, 707, and 735 K, respectively.

A. Data evaluation

After extracting the net intensities $I(006; \Psi; T)$ from the recorded ω -scan profiles, each resonance curve was fitted by a mixed Gaussian-Lorentzian-type function:

$$I(006; x) = \frac{a_0 \exp[-(1 - a_3)((x - a_1)/2a_2)^2]}{1 + a_3((x - a_1)/a_2)^2}, \quad (1)$$

where $x = E - E_a$. Thus, a_0 yielded the intensity maximum, a_1 the energy shift with respect to E_a , and a_2 is a measure of the full width at half maximum (FWHM) of the resonance. Since the intensities were not corrected for absorption the true resonance energies may be shifted towards somewhat lower values, which, however, is not important in the present context. An example of a resonance fit is given in Fig. 2, and energy as well as FWHM results are depicted in Fig. 3 showing that the resonance width (being dominated by the monochromator resolution) is practically invariant against T whereas the resonance energy experiences a significant decrease of about 1 eV upon raising the temperature from 299 to 735 K.

The maximum intensities exhibit a pronounced increase with increasing temperature. Combining the low-temperature results reported by Kokubun *et al.*⁴ with the refined a_0 values, both on a common arbitrary scale, provides a clear picture of the 006 intensity evolution over a wide temperature range between 30 and 735 K (Fig. 4).

III. THEORY

In this section, the phenomenological theory of the thermal-motion-induced reflections²⁻⁴ is further developed in

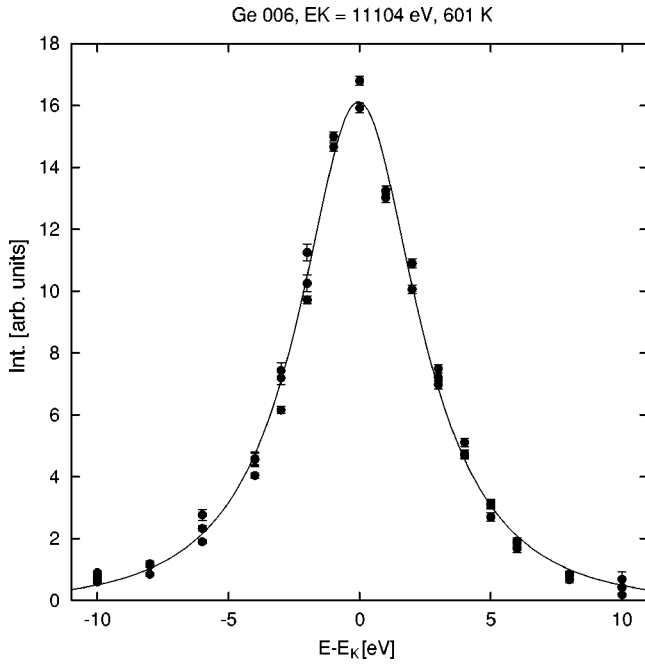


FIG. 2. Energy dependence of $I(006)$ at $T=601$ K, fit curve from Eq. (1).

order to take into account both optical and acoustical phonons in Ge. To this purpose we calculate the resonant tensor structure factor $F_{jk}(\mathbf{H})$ given by

$$F_{jk}(\mathbf{H}) = \sum_s \overline{f_{jk}(s) \exp(i\mathbf{H}\mathbf{r}^s)}. \quad (2)$$

Here and below, the bar denotes averaging over the thermal displacements $\mathbf{u}(s)$ of atoms (such as in the case of the Debye-Waller factor calculation). $\mathbf{u}(s) = \mathbf{r}^s - \mathbf{r}_0^s$, and \mathbf{r}^s and \mathbf{r}_0^s are the instantaneous and equilibrium positions, respectively, of the s th atom in the unit cell, $f_{jk}(s)$ is the tensor atomic form factor, and \mathbf{H} is the reciprocal-lattice vector of the reflection.

In the dipole approximation, the anisotropy of resonant scattering is described by the anisotropic part of the tensor

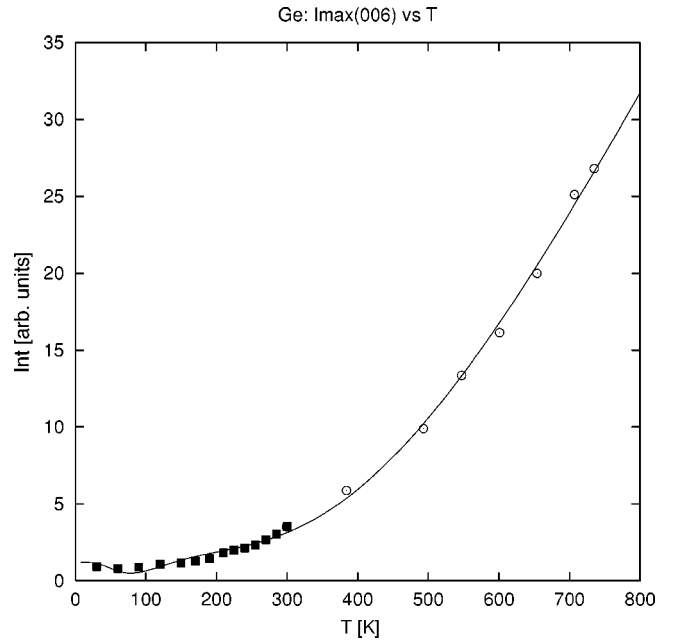
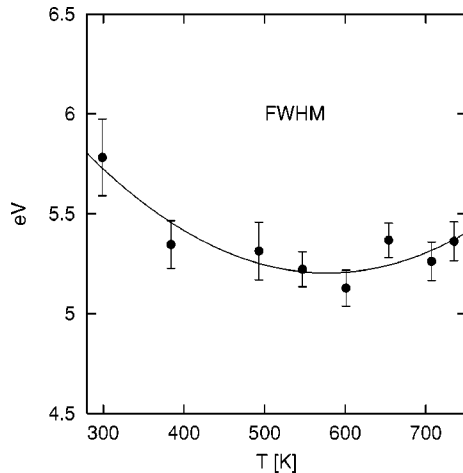


FIG. 4. Fitting of the 006 reflection intensity with Eq. 18. Circles with experimental bars—the present paper, squares—from Kokubun *et al.* (Ref. 4) The fitting curves are practically the same for two sets of fitting parameters discussed in the text.

form factor, f_{jk} , depending on the atomic environment and on the x-ray energy, E . If we neglect thermal motion, then $f_{jk} = 0$ due to the $\bar{4}3m$ symmetry of the undistorted atomic site in Ge. In order to find the thermal-motion-induced (TMI) anisotropy of $f_{jk}(s)$, we consider an atom (0) at the origin (000) of the diamond unit cell²⁵ so that its four next neighbors (1), (2), (3), and (4) are at the positions $(\frac{1}{4}\frac{1}{4}\frac{1}{4})$, $(\frac{1}{4}\frac{1}{4}\frac{3}{4})$, $(\frac{3}{4}\frac{1}{4}\frac{1}{4})$, and $(\frac{3}{4}\frac{1}{4}\frac{3}{4})$. A distortion of the atomic environment arises from both the thermal displacement of the atom itself, $\mathbf{u}(0)$, and from the displacements of its adjacent atoms, $\mathbf{u}(N)$. Obviously, only the relative displacements of the atoms are important for the distortion of the local environment, so that the anisotropy of the tensor form factor, f_{jk} , should be a function of $\mathbf{u}(N) - \mathbf{u}(0)$. Below, only

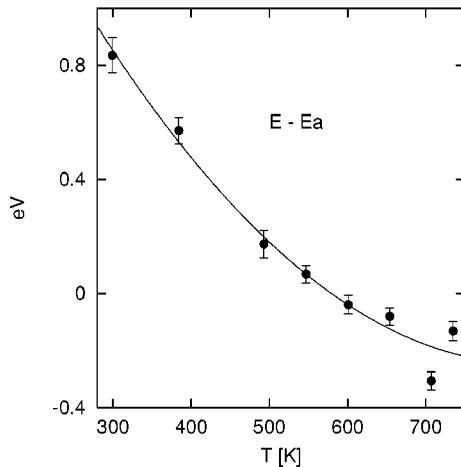


FIG. 3. Temperature dependence of the resonance FWHM (left) and of the resonance energy (right) for the 006 reflection.

the next four neighbors, which provide the greatest contributions to the anisotropy, will be considered, hence $N = 1, \dots, 4$. If the displacements are small, then the induced anisotropy will be small too, and we can use a phenomenological expansion for f_{jk} :

$$f_{jk}(0) = \sum_{N=1}^4 f_{jkm}(N)[u_m(N) - u_m(0)] + \dots, \quad (3)$$

where $f_{jkm}(N)$ is a partial derivative $\partial f_{jk}(0)/\partial u_m(N)$ taken at the equilibrium position, i.e., for $\mathbf{u}(0) = \mathbf{u}(1) = \mathbf{u}(2) = \mathbf{u}(3) = \mathbf{u}(4) = 0$. Higher-order terms are omitted because they add much smaller contributions² and may therefore be neglected. In Eq. (3) and below, the summation over repeated indices is assumed.

Assuming further that the scalar product $\mathbf{Hu}(s)$ is also small we can expand $\exp(i\mathbf{Hr}^s)$:

$$\exp(i\mathbf{Hr}^s) = \{1 + i\mathbf{Hu}(s) - \frac{1}{2}[\mathbf{Hu}(s)]^2 \dots\} \exp(i\mathbf{Hr}_0^s). \quad (4)$$

Multiplying Eqs. (3) and (4) and averaging over the temperature vibrations shows that we should know two tensor correlation functions, $\overline{u_m(0)u_n(0)}$ and $\overline{u_m(N)u_n(0)}$ (i.e., the autocorrelation and the correlation between the closest neighbors, respectively). The linear terms, $\overline{u_m(N)}$, obviously vanish. Owing to the $\bar{4}3m$ symmetry of the atomic positions we obtain $\overline{u_m(0)u_n(0)} = \overline{u_x(0)u_x(0)}\delta_{mn} = \frac{1}{3}\overline{u^2}\delta_{mn}$ where $\overline{u^2}$ is the mean-square displacement which can be assessed independently via the Debye-Waller factor of nonforbidden reflections. The tensors $\overline{u_m(N)u_n(0)}$ possess $3m$ symmetry and are symmetrical, $\overline{u_m(N)u_n(0)} = \overline{u_n(N)u_m(0)}$. Hence, all of them can be expressed using the tensor $\overline{u_m(1)u_n(0)}$ and the $\bar{4}3m$ symmetry operations. Therefore, there are only two independent components, $\overline{u_x(1)u_x(0)}$ and $\overline{u_y(1)u_x(0)}$. These components, as well as $\overline{u_x(0)u_x(0)}$, have been calculated as functions of temperature for silicon and germanium²⁰ employing the adiabatic bond charge model.

The third-rank tensors $f_{jkm}(N)$ are symmetrical over the first two indices, $f_{jkm}(N) = f_{kjm}(N)$. They also possess $3m$ symmetry and should therefore have four independent components.²⁶ All the tensors are related to $f_{jkm}(1)$ by the $\bar{4}3m$ symmetry operations. Considering $f_{jkm}(1)$, none of its 27 components is vanishing, and since the threefold axis is directed along $[111]$, the tensor should be invariant against circular permutation of x , y , and z . In addition, due to the diagonal mirror planes the tensor should also be invariant against permutations $x \leftrightarrow y$, $z \leftrightarrow z$, etc. Thus, as a result of all this permutations one finds

$$f_{xxx} = f_{yyy} = f_{zzz}, \quad (5)$$

$$f_{xyz} = f_{yzx} = f_{zxy}, \quad (6)$$

$$f_{xxy} = f_{xxz} = f_{yyx} = f_{yyz} = f_{zxx} = f_{zzy}, \quad (7)$$

$$f_{xyx} = f_{xyy} = f_{yzy} = f_{yzz} = f_{zxx} = f_{zxx}, \quad (8)$$

and one can take f_{xxx} , f_{xyz} , f_{xxy} , and f_{xyx} as the four independent components.

After averaging over the temperature vibrations, Eqs. (3) and (4) yield for atom (0)

$$\begin{aligned} \overline{iH_n u_n(0) f_{jk}(0)} &= 4i \{ f_{xyz} [\overline{u_x(1)u_x(0)} - \overline{u_x^2(0)}] \\ &\quad + 2f_{xyx} \overline{u_x(1)u_y(0)} \} T_{jkn} H_n, \end{aligned} \quad (9)$$

where T_{jkn} is the only third-rank tensor possible for the $\bar{4}3m$ point symmetry.^{17,26} T_{jkn} is symmetrical over all its indices, i.e., $T_{xyz} = T_{yzx} = T_{zxy} = T_{xzy} = T_{zyx} = T_{yxz} = 1$, and all other components with at least two coinciding indices vanish. Exactly the same result is obtained for the other three atoms in the unit cell, which are related to atom (0) by the face-centering operations. For the remaining four atoms in the unit cell, the tensor T_{jkn} changes sign since these atoms are related to atom (0) by the inversion operation. For the hkl ($h+k+l=4n+2$) ‘‘forbidden’’ reflections, this change of sign is exactly compensated by the phase factor $\exp(i\mathbf{Hr}_0^s) = -1$ [see Eq. (4)]. Thus, for the $0kl$ ($k+l=4n+2$) ‘‘forbidden’’ reflections, the tensor contribution to the tensor structure amplitude is the same for all eight atoms in the unit cell, and we finally obtain

$$\begin{aligned} F_{jk}(\mathbf{H}) &= 32i \{ f_{xyz} [\overline{u_x(1)u_x(0)} - \overline{u_x^2(0)}] \\ &\quad + 2f_{xyx} \overline{u_x(1)u_y(0)} \} T_{jkn} H_n \exp[-(\overline{\mathbf{Hu}})^2/2]. \end{aligned} \quad (10)$$

Thus, we see that only two independent components of four, f_{xyz} and f_{xyx} , give contributions to the structure amplitudes of the ‘‘forbidden’’ reflections. The structure factor tensor has the same form as in the dipole-quadrupole theory,¹⁷ however, in our case, it varies proportionally to the displacement-displacement correlation functions and thus strongly depends on the temperature.

In Eq. (10), the Debye-Waller factor, $\exp[-(\overline{\mathbf{Hu}})^2/2]$, is added just for physical reasons. It is easy to prove that this factor appears for the term proportional to $\overline{u_x(0)u_x(0)}$. Indeed, we can use

$$\begin{aligned} \overline{u_x \exp(i\mathbf{Hu})} &= -i \frac{\partial [\overline{\exp(i\mathbf{Hu})}]}{\partial H_x} \\ &= -i \frac{\partial \{ \exp[-(\overline{\mathbf{Hu}})^2/2] \}}{\partial H_x} \\ &= i H_x \overline{u_x} \exp[-(\overline{\mathbf{Hu}})^2/2]. \end{aligned} \quad (11)$$

In other words, there is no need to use the expansion (4) for this term and we can calculate it for any temperature, even if $(\overline{\mathbf{Hu}})^2$ is not small. The same result can be directly obtained using the Wick theorem for the statistical average of the Bose-type operators²⁷ (but the calculations are more tedious). As a nontrivial consequence of the Wick theorem one can see that for any operator w , which is proportional to phonon displacements, the statistical average yields

$$\overline{w \exp(i\mathbf{Hu})} = i H_k \overline{w u_k} \exp[-(\overline{\mathbf{Hu}})^2/2]. \quad (12)$$

Therefore, we should use the Debye-Waller factor for all the terms in Eq. (10).

If the displacements of the neighboring atoms were equal (such as in acoustical-phonon modes with small wave vectors), then we would have $u_x(1)u_y(0) = 0$ and $u_x(1)u_x(0) = u_x(0)u_x(0)$ so that these modes would not contribute to the “forbidden” reflections. However, the numerical simulations show²⁰ that the displacements are never equal, even for $T=0$.

Equation (10) can be rewritten using the invariant correlations, u_{\parallel}^2 and u_{\perp}^2 , parallel and perpendicular to the covalent bonds, i.e., $[\mathbf{u}(1) - \mathbf{u}(0)]^2 = u_{\parallel}^2 + u_{\perp}^2$. Then, taking into account that

$$u_{\parallel}^2 = 2\overline{u_x^2(0)} - \overline{2u_x(1)u_x(0)} - 4\overline{u_x(1)u_y(0)}, \quad (13)$$

$$u_{\perp}^2 = 4\overline{u_x^2(0)} - 4\overline{u_x(1)u_x(0)} + 4\overline{u_x(1)u_y(0)}, \quad (14)$$

we obtain from Eq. (10)

$$F_{jk}(\mathbf{H}) = -\frac{16}{3} i [u_{\perp}^2 f_{\perp} + u_{\parallel}^2 f_{\parallel}] T_{jkn} H_n \exp[-\overline{(\mathbf{H}\mathbf{u})^2}/2], \quad (15)$$

where $f_{\perp} = f_{xyz} - f_{xyx}$ and $f_{\parallel} = 2f_{xyx} + f_{xyz}$.

The observed intensity of a “forbidden” reflection is proportional to $|F|^2/\mu$ where μ is the absorption coefficient (in spite of the high perfection of Ge crystals one can use the kinematical approximation because the structure amplitudes are very small). The slight temperature dependence of μ is ignored below.

IV. FITTING PROCEDURE

In principle, the considered effect can be used to study the phonon-electron interaction [f_{xyx} and f_{xyz} in Eq. (15)] and the temperature dependencies of the relative displacements u_{\parallel}^2 and u_{\perp}^2 . The aim of the present paper is restricted to demonstrating that the observed intensity of the 006 reflection can be quantitatively described by the theory.

For Ge, both u_{\parallel}^2 and u_{\perp}^2 have been measured by the extended-x-ray-absorption fine-structure (EXAFS) method,²⁸ however with considerable uncertainties, especially for u_{\perp}^2 . Therefore, we use the theoretical values of u_{\parallel}^2 and u_{\perp}^2 given in Ref. 20 which are in good agreement with the experimental data. Unfortunately, these theoretical values were calculated only up to 500 K and there is no u_{\perp}^2 for Ge, only for Si (but the authors claimed that the data for Si and Ge are very similar when proper temperature scaling is taken into account).²⁰ Hence, the temperature dependence of u_{\perp}^2 was derived for Ge using the available data for u_{\parallel}^2 and the Si data for $u_x(1)u_y(0)$, with the temperature divided by a factor 1.7. In this way, the numerical values of u_{\perp}^2 and u_{\parallel}^2 were obtained for the relevant temperature interval. However, for the fitting procedure, it is more convenient to use analytical expressions for the temperature dependence of u_{\parallel}^2 and u_{\perp}^2 . It is found from Ref. 20 that within a few percent (good enough for our purposes) both u_{\parallel}^2 and u_{\perp}^2 can be described by the Einstein formulas

$$u_{\parallel}^2 = u_{\parallel 0}^2 \coth\left(\frac{\hbar \omega_{\parallel}}{2kT}\right), \quad (16)$$

$$u_{\perp}^2 = u_{\perp 0}^2 \coth\left(\frac{\hbar \omega_{\perp}}{2kT}\right), \quad (17)$$

with $u_{\parallel 0}^2 = 0.00178 \text{ \AA}^2$, $u_{\perp 0}^2 = 0.00574 \text{ \AA}^2$, $\omega_{\parallel} = 7.21 \text{ THz}$, and $\omega_{\perp} = 3.74 \text{ THz}$.

For the Debye-Waller factor, the high-temperature dependence, known from literature, is used: $\overline{(\mathbf{H}\mathbf{u})^2} = AT$ where $A = 0.001068 \text{ K}^{-1}$. For low temperatures (less than 100 K), there is a deviation from the linear dependence²⁰ (but then, the Debye-Waller corrections are negligibly small).

In Eq. (15), the complex parameters f_{xyx} and f_{xyz} should be considered as independent so that for the measured intensity proportional to $|F|^2$ there are three fitting parameters. However, fits of the observed intensities by Eq. (15) and the use of these three parameters are not satisfactory. A possible reason is that the structure factor may also contain a temperature-independent contribution caused by several possible effects such as dipole-quadrupole scattering,¹⁷ defect-induced distortions,³ and/or multiple-wave contributions (Renning effect). In the first two cases, the tensor form of the additional term is exactly the same as for the temperature-induced one. In the case of a significant multiple-wave contribution, the tensor form and hence the corresponding polarization properties would be different from Eq. (15). Though we have tried to minimize the influence of multiple scattering by measuring at different azimuthal angles, we cannot completely rule out small effects because the polarization properties of the 006 reflection were not studied.

Finally, the intensity was fitted to the expression

$$I(T) = \left\{ \left[C' + P_{\perp} \coth\left(\frac{\hbar \omega_{\perp}}{2kT}\right) + P'_{\parallel} \coth\left(\frac{\hbar \omega_{\parallel}}{2kT}\right) \right]^2 + \left[C'' + P''_{\parallel} \coth\left(\frac{\hbar \omega_{\parallel}}{2kT}\right) \right]^2 \right\} \exp(-AT), \quad (18)$$

where the five fitting parameters are given by

$$P_{\perp} = u_{\perp 0}^2 |f_{\perp}|, \quad (19)$$

$$P'_{\parallel} = u_{\parallel 0}^2 |f_{\parallel}| \cos(\phi_{\perp\parallel}), \quad (20)$$

$$P''_{\parallel} = u_{\parallel 0}^2 |f_{\parallel}| \sin(\phi_{\perp\parallel}), \quad (21)$$

$$C' = |C| \cos(\phi_{\perp C}), \quad (22)$$

$$C'' = |C| \sin(\phi_{\perp C}), \quad (23)$$

so that $\phi_{\perp\parallel}$ is the phase between the two complex parameters, f_{\parallel} and f_{\perp} , while $\phi_{\perp C}$ is the phase between f_{\perp} and the temperature-independent contribution C . Since only relative intensities were measured, these five parameters can obviously be determined only on an arbitrary scale. The result of simultaneously fitting both the low-temperature and the elevated-temperature data is depicted in Fig. 4, while our new data alone, smoothed and extrapolated up to the melting

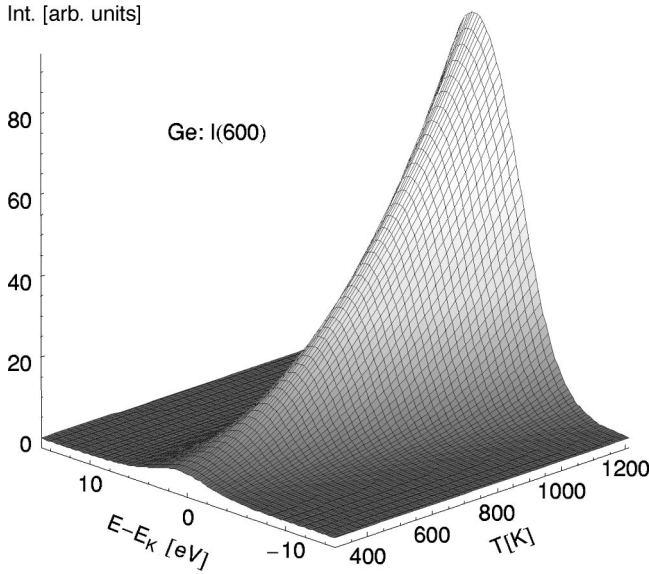


FIG. 5. The 006 reflection intensity vs energy and temperature. The extrapolation up to the melting temperature shows an almost 60-times increase in the whole temperature interval.

temperature, are presented in Fig. 5. Note that the fit curve in Fig. 4 would be the same if the signs of $\phi_{\parallel\perp}$ and $\phi_{\perp C}$ were simultaneously changed.

V. DISCUSSION

Figure 4 shows that it is possible to describe the temperature dependence for the whole investigated temperature interval by only a few (five) parameters. Unfortunately, these parameters are not unambiguous. Two different sets of parameters yield practically undistinguishable temperature dependencies (Fig. 4). These sets are rather different (errors in parentheses), for set I, $C' = 6.11(42)$, $C'' = -0.81(36)$, $P_{\perp} = 4.86(65)$, $P'_{\parallel} = -11.84(1.24)$, and $P''_{\parallel} = 1.50(18)$, whereas for set II, $C' = 5.59(55)$, $C'' = -3.29(25)$, $P_{\perp} = 5.31(55)$, $P'_{\parallel} = -11.68(1.29)$, and $P''_{\parallel} = 2.50(8)$.

Such an ambiguity arises, perhaps, from the very similar temperature behaviors of the two vibration modes, u_{\parallel}^2 and u_{\perp}^2 , i.e., they are constant at low temperatures and proportional to T for high temperatures. Another consequence of this similarity is that $I(T)$ is not very sensitive to the phonon frequencies. Practically the same fitting can also be obtained if one accepts the experimental values $\omega_{\parallel} = 7.55$ THz and $\omega_{\perp} = 3$ THz found from the EXAFS data.²⁸ In spite of this ambiguity we can, however, conclude that the parallel displacement is more effective in producing the anisotropy than is the perpendicular displacement. Indeed, the ratio $|f_{\parallel}/f_{\perp}| = \sqrt{P'_{\parallel} + P''_{\parallel} u_{\perp 0}^2 / (P_{\perp} u_{\parallel 0}^2)}$ is large, 7.92 for set I and 7.2 for set II, respectively. Then, as can be expected from the physics of the phenomenon, the parallel and perpendicular displacements produce anisotropies of almost opposite signs so that $\cos \phi_{\parallel\perp}$ is negative and large in absolute value ($\cos \phi_{\parallel\perp}$ is approximately -0.99 for set I and -0.98 for set II).

Another problem is related to the physical interpretation of the fitting. Indeed, both the temperature-induced and the

temperature-independent terms in the intensity are very large (note that the temperature-induced term includes the quantum vibrations at $T=0$). However, the interference term is negative (and also large in absolute value), and it almost compensates the first two. In other words, in the structure factor, the temperature-induced and the temperature-independent terms almost compensate each other at low temperatures (i.e., the absolute value of $C' + P_{\perp} + P'_{\parallel}$ is small in comparison to the absolute values of the individual terms of the sum). This situation seems rather strange from the physical point of view, but there may be several explanations:

(i) The zero- T quantum vibrations give no contribution to the TMI anisotropy. This point is related to the problem of quantum measurements and this is obviously beyond the scope of present paper.

(ii) The next-neighbor contributions to the TMI anisotropy, though it is rather doubtful that they could effect much because their temperature dependence is similar to that of the first-neighbor contribution.

(iii) Higher-order contributions (for example, of, say, u^4 , which is proportional to T^2). Though the T^2 term in the structure amplitude nicely fits the intensity data, from the physical point of view, it is still not clear why this term should be taken into account.

(iv) A very strong temperature dependence of the electron density of states right near the absorption edge. Such a strong dependence should, however, also be observed for normal absorption, which does not seem to be the case.

VI. CONCLUSION

In comparison with previous work,²⁻⁴ the theory of TMI reflections is improved by a systematic consideration of both parallel and perpendicular correlations in the displacements of neighboring atoms. It is shown that two complex parameters, $2f_{xyx} + f_{xyz}$ and $f_{xyz} - f_{xyx}$, connect the induced x-ray anisotropy with the parallel and perpendicular correlations, u_{\parallel}^2 and u_{\perp}^2 , respectively. The theory is, however, still far from a desirable state. The present phenomenological approach should be accompanied, if possible, by quantum-mechanical calculations, similar to those used for x-ray absorption.²⁹⁻³² This would allow a better understanding of the phonon-electron interaction in solids. For example, in spite of the above-mentioned ambiguity we can conclude that the parallel displacements are more efficient than the perpendicular ones in producing the anisotropy since the obtained $|2f_{xyx} + f_{xyz}|$ is significantly larger than $|f_{xyz} - f_{xyx}|$.

Experimentally, it would be very important to study the TMI reflections with sub-eV resolution in order to obtain a more detailed picture of the temperature dependence of the energy spectra. For improving the accuracy, the measurements should also be done with one and the same sample, from low temperatures up to the melting point, and the intensities should be calibrated with respect to nonforbidden reflections. It would also be very interesting to know whether the theory holds near the melting point where the vibrations have maximum amplitudes. Another important parameter, the phase of the TMI structure factor (i.e., the absolute phases of both $2f_{xyx} + f_{xyz}$ and $f_{xyz} - f_{xyx}$), could be as-

sessed via interference with the “umweganregung” of non-forbidden reflections.

In conclusion, for a germanium single crystal, we have observed the thermal-motion-induced 006 reflection at temperatures between 299 and 735 K. In this interval, the intensity increases almost eight times. Combining our data with the recent low-temperature data of Kokubun *et al.*⁴ it is shown that the whole temperature evolution of the “forbidden” reflection 006 can be theoretically described, assuming that the thermal-motion-induced anisotropy of x-ray suscep-

tibility is proportional to the relative displacements of neighboring atoms.

ACKNOWLEDGMENTS

Fruitful discussions with E.N. Ovchinnikova and M.B. Mensky are acknowledged. This work was supported by the Bundesminister für Bildung und Forschung (BMBF Contract No. 05 KS1PDA) and partly by the INTAS Grant 01-0822.

-
- ¹N. W. Ashcroft and N. D. Mermin, *Solid State Physics* (Holt, Rinehart and Winston, New York, 1976), Vol. 2.
- ²V.E. Dmitrienko, E.N. Ovchinnikova, and K. Ishida, *Pis'ma Zh. Éksp. Teor. Fiz.* **69**, 885 (1999) [*JETP Lett.* **69**, 938 (1999)].
- ³V.E. Dmitrienko and E.N. Ovchinnikova, *Acta Crystallogr., Sect. A: Found. Crystallogr.* **A56**, 340 (2000).
- ⁴J. Kokubun, M. Kanazawa, K. Ishida, and V.E. Dmitrienko, *Phys. Rev. B* **64**, 073203 (2001).
- ⁵R. Colella (private communication).
- ⁶D.H. Templeton and L.K. Templeton, *Acta Crystallogr., Sect. A: Found. Crystallogr.* **36**, 237 (1980).
- ⁷V.E. Dmitrienko, *Acta Crystallogr., Sect. A: Found. Crystallogr.* **39**, 29 (1983).
- ⁸V.E. Dmitrienko, *Acta Crystallogr., Sect. A: Found. Crystallogr.* **40**, 89 (1984).
- ⁹D.H. Templeton and L.K. Templeton, *Acta Crystallogr., Sect. A: Found. Crystallogr.* **41**, 133 (1985).
- ¹⁰D.H. Templeton and L.K. Templeton, *Acta Crystallogr., Sect. A: Found. Crystallogr.* **42**, 478 (1986).
- ¹¹K. Eichhorn, A. Kirfel, and K. Fischer, *Z. Naturforsch., A: Phys. Sci.* **43a**, 391 (1988).
- ¹²A. Kirfel, A. Petkov, and K. Eichhorn, *Acta Crystallogr., Sect. A: Found. Crystallogr.* **47**, 180 (1991).
- ¹³D.H. Templeton and L.K. Templeton, *Acta Crystallogr., Sect. A: Found. Crystallogr.* **48**, 746 (1992).
- ¹⁴A. Kirfel, T. Lippmann, and W. Morgenroth, *HASYLAB Jahresberichte*, p. 371 (1995).
- ¹⁵T. Nagano, J. Kokubun, I. Yazawa, T. Kurasawa, M. Kuribayashi, E. Tsuji, K. Ishida, S. Sasaki, T. Mori, S. Kishimoto, and Y. Murakami, *J. Phys. Soc. Jpn.* **65**, 3060 (1996).
- ¹⁶Y. Murakami, H. Kawada, H. Kawata, M. Tanaka, T. Arima, Y. Moritomo, and Y. Tokura, *Phys. Rev. Lett.* **80**, 932 (1998).
- ¹⁷D.H. Templeton and L.K. Templeton, *Phys. Rev. B* **49**, 14 850 (1994).
- ¹⁸A. Kirfel and H.-G. Krane, *HASYLAB Jahresberichte*, p. 567 (1999).
- ¹⁹A. Kotani and S. Shin, *Rev. Mod. Phys.* **73**, 203 (2001).
- ²⁰O.H. Nielsen and W. Weber, *J. Phys. C* **13**, 2449 (1980).
- ²¹J. Kulda, D. Strauch, P. Pavone, and Y. Ishii, *Phys. Rev. B* **50**, 13 347 (1994).
- ²²M. Wendschuh-Josties and R. Wulf, *J. Appl. Crystallogr.* **22**, 282 (1989).
- ²³See [www-hasylib. desy. de/facility/experimentalstations/stations/d](http://www-hasylib.desy.de/facility/experimentalstations/stations/d)
- ²⁴C. Scheufler, V. Engel, and A. Kirfel, *J. Appl. Crystallogr.* **30**, 411 (1997).
- ²⁵*International Tables for Crystallography*, edited by T. Hahn (Kluwer Academic, Amsterdam 1996), Vol. A.
- ²⁶Yu. Sirotnin and M.P. Shaskolskaya, *Fundamentals of Crystal Physics* (Mir, Moscow, 1982).
- ²⁷L.D. Landau and E. M. Lifshitz, *Electrodynamics of Continuous Media* (Pergamon, New York, 1980), Chap. XVI.
- ²⁸G. Dalba, P. Fornasini, R. Grisenti, and J. Purans, *Phys. Rev. Lett.* **82**, 4240 (1999).
- ²⁹J.J. Rehr and R.C. Albers, *Rev. Mod. Phys.* **72**, 621 (2000).
- ³⁰J. García, G. Subías, M.G. Proietti, H. Renevier, Y. Joly, J.L. Hodeau, J. Blasco, M.C. Sánchez, and J.F. Bérrar, *Phys. Rev. Lett.* **85**, 578 (2000).
- ³¹P. Benedetti, J. van den Brink, E. Pavarini, A. Vigliante, and P. Wochner, *Phys. Rev. B* **63**, 060408(R) (2001).
- ³²Y. Joly, *Phys. Rev. B* **63**, 125120 (2001).